Additive Manufacturing of Phase-Change Material Suspended in Photocurable Resin for Thermal Energy Storage

Caleb J. Collins*
University of Tennessee, Knoxville, TN, 37996

The goal of this study is to build upon previous research in the suspension of microencapsulated phase-change material (MEPCM) in photocurable resin with the intention of additively manufacturing heat exchangers capable of storing large amounts of latent heat for thermal energy storage (TES) applications. Liquid crystal display ((LCD) printing methods were used with the intention of creating enhanced geometrical features, including a high surface-area-to-volume ratio, thin fins/walls, and uniform PCM suspension across the geometry. To solve issues with the viscosity of the MEPCM-resin composites, methods involving heating the composite material, the resin vat, and printing bed were experimented with to determine if the resulting samples were of better quality in both TES capabilities and geometrical stability. The thermal properties of the resulting composite samples were analyzed and compared to bulk materials and previous findings. Dimensional analysis was also performed on the samples to determine the quality and resolution of the composite prints. Although the LCD 3D printing process of the MEPCM=resin mixtures provided lower amounts of complications compared to other techniques used, there is a very crucial limiting factor that currently prevents higher MEPCM ratios from being obtained. The composite resins heated in this study showed that the heated process and techniques lead to more efficient and effective printing and increased latent heat of fusion and thermal conductivity, vital qualities needed for TES.

Nomenclature

d	=	depth, mm
h_{sl}	=	Latent Heat of Fusion, $kJ \cdot kg^{-1}$
k	=	Thermal Conductivity, $W \cdot m^{-1} \cdot K^{-1}$
L	=	Length, mm
T	=	Temperature, °C
t	=	thickness, mm
W	=	Width, mm

I. Introduction

Phase-change materials (PCMs) have become relevant to a large extent when attempting to optimize the use of thermal energy due to their ability to absorb substantial amounts of energy in the form of heat as they undergo a phase change remaining at a mostly constant temperature. This attribute makes PCMs ideal for thermal energy storage (TES) and control in a large number of applications including thermal management of buildings [1–4], refrigeration of perishables[5–7], and biomedical applications [8–10].

There are multiple different types of PCMs, all with their own specific set of advantages and disadvantages. For TES, the selected PCM should have a high latent heat, high thermal conductivity, chemical stability, low cost, and be nonflammable [11, 12]. However, organic PCMs (e.g., bio-based, paraffins, and fatty acids), that are flammable and possess low thermal conductivity, have been found to be the most used materials TES [13, 14]. Organic PCMs have been extensively researched and are extensively used in TES because of their large range of transition temperatures in addition to their chemical stability, thermal stability, and low toxicity. As PCMs go through thermal cycling in their respective applications, the material continuously cycles between its solid and liquid phase. Using a microencapsulated form of PCM has been found to mitigate this issue, allowing for higher PCM retention and improving system longevity [15–17].

*REU Student Intern, Department of Aerospace Engineering, Student Member 1538821 - Undergraduate Category

Introducing additive manufacturing techniques to the production of PCM-based TES systems can help magnify the heat transfer characteristics of the PCMs by allowing for complex geometries that were previously found to be unfeasible when using more traditional methods, such as injection molding and casting [18]. The geometrical complexities possible with additive manufacturing result in high surface-area-to-volume ratios, optimized PCM content, and walls that are more slender but still have structural stability, all of which actively enhance the execution of heat transfer within the system. The utilization of these techniques also allows for the implementation of materials that were seen as atypical for thermal applications in previous years. While metal heat exchangers have been seen as the standard for many years, polymer heat exchangers have begun to gain traction in the field due to multitude of advantages they provide. Contrary to their metal counterparts, polymer heat exchangers are low in weight and cost, antifouling, and anticorrosive [19, 20]. Another advantage to polymers is that they possess low melting points and require low processing temperatures, implicating that they require less energy to manufacture than the metal equivalents [21]. Some of the limitations to using polymers, inclusive but not limited to their low thermal conductivity, could be mitigated in the design process by introducing slender walls [22, 23] or thermal conductivity enhancing additives such as expanded graphite [24], graphene [25], carbon nanotubes [26], and ceramic fillers [27].

A few of the additive manufacturing techniques that are being explored for the 3D printing of PCM composites are filament-extrusion-based such as fused filament fabrication (FFF), also known as fused filament deposition (FDM) [28–32]. Comparably, another additive manufacturing technique that is being used in these applications is direct ink writing (DIW) [33–36], which relies on the depositing of an ink through a layer-by-layer extrusion similar to that of FDM or FFF. Resin-based processes such as stereolithography (SLA), digital light processing (DLP), and liquid crystal display (LCD) are also being used to fabricate PCM-based structures [37–39]. These manufacturing processes function by exposing a layer of photocurable resin to a UV light source or laser, determined by the method in use. The resultant 3D printed geometries have been found to have very high resolution in relatively short time frames compared to other techniques.

Currently FFF and FDM continue to be very popular in the field due to the low cost involved with the materials and associated equipment, wide variety of material options, and the overall ability to scale [32, 40]. This technique however involves the fabrication of a custom composite filament that can be very difficult to achieve consistent samples [29, 32]. Additionally, the elevated temperatures involved in the filament extrusion process have been found tp compromise the integrity of the encapsulation shells or result in low PCM retention during fabrication. These filament-dependent techniques have been found to also result in large air gaps in the 3D printed parts, causing an increase in the thermal resistance that is found between the print layers, decreasing the overall effective thermal conductivity of the component [41].

Previous work by researchers at Embry Riddle Aeronautical University Daytona Beach [42] suspended MEPCM in a photocurable resin for LCD 3D printing of composites possessing the capability of TES. The thermal properties of the resulting sample composites, comprised of different mass ratios of MEPCM to photocurable resin, were studied to determine the TES capability and thermal conductivity using differential scanning calorimetry (DSC) and transient plane source (TPS), respectively. The highest ratio, 37% MEPCM, was found to have an effective PCM content of 32.47%, indicating a relatively smaller PCM loss than some of the other methods studied. The primary issue found within the study was that as the ratio of MEPCM went up, the viscosity of the composite resin became too high for creating reliable and efficient prints.

In the current study, the composite resin and the 3D printing bed is heated to lower the viscosity, in order to achieve more reliable prints. Room Temperature samples would be made of different ratios, 25%, 30%, and 35%, along with samples made when the composites are heated to 65 °C. These would then be studied for their TES capabilities using DSC and TPS. Additionally, using microscopic imaging, the surface and cross-sectional microstructures of the samples were visualized to verify the general material distribution and the state of the capsule shells post printing and processing. The goal of this study is to determine the thermal properties of the resulting MEPCM/resin samples, such as latent heat of fusion, phase-change temperature, and thermal conductivity while also verifying the ability to print complex geometries to assist in the efficiency of the storage of thermal energy.

II. Materials and Manufacturing Methods

A. Materials

The photocurable resin, High Tensile UV Photopolymer, was supplied by Photocentric (Avondale, AZ). The technical data sheet provided by Photocentric reports a heat deflection temperature of 63 °C, a density of 1.16 g/cm^3, and a

viscosity of 510 cPs. The microencapsulated PCM, EnFinit PCM 28RPS-T, was supplied by Encapsys (Appleton, WI) and has a manufacturer-reported phase-change temperature of 28 °C.

B. Manufacturing Equipment

Multiple Liquid Crystal Display Resin 3D Printers from ELEGOO (Shenzhen, China), Mars 3, Mars 2 Pro, and Saturn 3 Ultra were used to manufacture samples for testing. To test the differences in manufacturing with printing samples at room temperature and at an increased temperature of 65 °C, multiple 12W Flexible Polyimide Heater Plates from Harissess were adhered to both the resin vat and build plate. The resin vat and bed were both heated to 65 °C when heating the resin before printing. Once the samples had begun to be printed, the bed was set to 50 °C.

C. Mixture Preparation

Differing mixtures of resin and MEPCM were created by combining the two materials to form specific mass ratios. Mixing was done manually with low intensities and speeds to prevent shell fractures as a result from stirring. Since varying the amount of PCM in the composite directly correlates to the TES capacity, maximizing the amount of PCM within the composite is a priority; however, 3D printing methods that use photocurable resin as a printing medium are especially sensitive to variations in the resin properties such as its viscosity and depth of penetration. Altering these properties by introducing additives such as the MEPCM can affect the resin curability and cause the printing process to fail. The MEPCM ratios outlined in this study are 0%, 25%, 30%, and 35%. Mixtures that were to be used for created using the Heated Printer were placed in an isotemp oven (Isotemp 737F Oven, Fisher Scientific, Waltham, MA) at 68 °C for at least 12 hours to pre-heat before being introduced to the heated vat.

III. Experimental Methods

A. Differential Scanning Calorimetry

A DSC (DSC 3 STARe, Mettler Toldeo, Columbus, OH) was used to measure the latent heats of fusion and phase-change temperatures of the MEPCM/Resin composite samples. Additionally, the effective amount of MEPCM was calculated using the latent heat of fusion. The masses of the samples, ranging between 12 and 18 mg were measured using an analytical balance (XS105DU, Mettler Toledo, Columbus, OH) before placing them in 40 µL aluminum crucibles. Each of the samples contained in the crucibles were held at an initial temperature of 0∘C for a 10 min duration. Then, the temperature was increased from 0∘C to 60 ∘C using a heating rate of 2 ∘C/min. The sample temperature of 60∘C was maintained for 10 min before being cooled to 0 ∘C at -2 ∘C/min. During this process, the heatflow and temperature were recorded every one second. These cycles were performed twice for each sample to ensure the material melted down and optimal thermal contact with the bottom of the crucible was achieved.

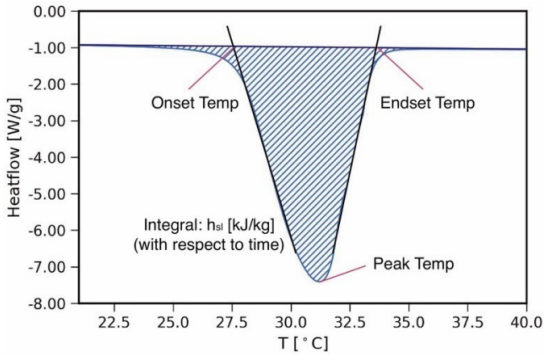

Fig. 1 Diagram illustrating heatflow versus temperature curve with labeled onset, endset, and peak temperatures in addition to the latent heat of fusion. The phase chnage temperature of the MEPCM suspended in the resin is represented by the peak.

Using the heatflow versus temperature curve obtained from the DSC testing, similar to the example graph seen in Fig. 1, the melting temperature range of the composite can be evaluated from the onset and endset temperatures. These are the temperatures at which the composite material begins and ends the melting phase. Graphically, the onset and endset temperature can be defined as the intersection between the tangents of the leading and trailing edge of the peak and baseline, respectively. The latent heat of fusion can also be determined in similar fashion and is defined as the integral or area under the heatflow versus temperature curve.

As an additional method to verify MEPCM distribution, samples from the edge and center locations were tested to ensure that the MEPCM was evenly distributed across the printed samples. This sample location study found that the latent heats of fusion varied by less than 2% across the two sampling locations used for each of the five samples tested.

B. Thermal Conductivity Measurements

Thermal conductivity measurements of the 3D-printed composites were taken using a thermal constants analyzer (Transient Plane Source (TPS) 2500S, Hot Disk, Gothenburg, Sweden). A 4-mm diameter Kapton sensor (C7577, Hot Disk, Gothenburg, Sweden), comprised of a resistance heater and a temperature sensor, was sandwiched between two 30-mm diameter 3D printed samples with a thickness of 5-mm. By applying Joule heating, the temperature response of the sensor can be used to determine the thermal conductivity of the samples through a mathematical model. A power of 5 mW and a sampling time of 10 seconds were used during testing, with each measurement being taken after a 30 minute standby time.

C. Print Quality and Resolution

A standard 3D-pinting "torture test" model, displayed in figure 2, was created using Solidworks 2022 (Dassault Systemes SolidWorks Corporation), a Computer-Aided Design (CAD) Software. Samples of the model was printed in the base resin and in a 25% MEPCM-resin composite. The resolution of the prints were compared to each other and the original CAD model. Measurements were taken of the sample size and the different geometrical tests and the average error was calculated to determine the quality and accuracy of the print. These geometrical features consist of a set of cubes and spheres of increasing size, a free standing arch, created using rectangular segments of 2 mm stacked on top of each other at 10 °, and different size thru-holes.

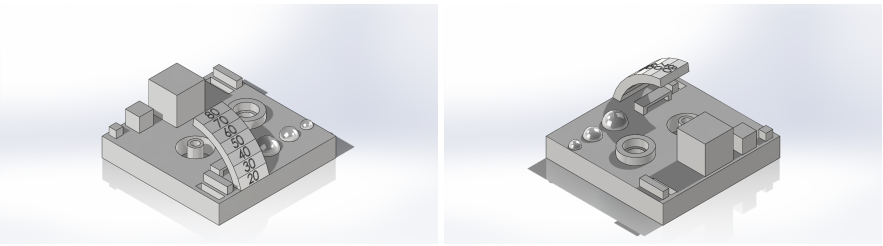

Fig. 2 CAD renderings of the torture test print.

IV. Results and Discussion

A. Phase-Change Temperature and Latent Heat of Fusion

As stated previously, samples were collected from edge and center locations to verify the general material distribution as a result of the mixture preparation and printing process. Throughout the sample preparation process, it was observed that the viscosity of the prepared MEPCM-resin mixture allowed for consistent suspension of the MEPCM even after periods of minimal mixing. As stated, the previous studies found that there was less than 1% latent heat of fusion variance across the five tested samples, indicating that the material distribution is fairly uniform across the radius of the samples. Following the sample location independence study, samples were taken from the midpoint to measure the phase-change peak temperature (Tpeak), onset temperature (Tonset), endset temperature (Tendset), and latent heat of fusion (hsl). Representative results for all explored MEPCM mass ratios are shown in Table 1. As an approach to obtain the effective MEPCM content in the post-processed samples, the ratio of the latent heats of fusion of the MEPCM/Resin samples and the pure MEPCM is determined. As shown in Table 1, there exists a discrepancy between the hypothesized

value and the actual value determined by the DSC testing. These losses can be attributed to a number of factors such as ruptured encapsulation shells that occur during the sample preparation process and/or chemical interactions between the materials and rinsing solvents. Prior work done by the authors using PureTemp (Minneapolis, MN) PCM42 and HDPE as a shape stabilizer had a considerably higher loss of PCM during the fabrication process [28, 29]. In these studies, the PCM/HDPE composite was extruded into custom filament to be used in FFF 3D printing. These manufacturing processes involve prolonged exposure to high temperatures and stresses which results in the leaking of PCM as is reflected in the lower latent heat of fusion of the final product. The higher PCM retention rate provided by the encapsulation material and minimal thermal stresses imposed by the manufacturing process results in a significant improvement in the containment of PCM. In the current study, 35% was the highest achievable content of MEPCM that still results in a mixture suitable for effiecent additive manufacturing and provides the effective TES capacity of a composite containing 31.51% MEPCM.

Table 1 Phase-change temperature and latent heat of fusion for differing samples of MEPCM-Resin material.

		T_{peak} ($°C$)	T_{onset} ($°C$)	T_{endset} ($°C$)	h_{sl} (kJ/kg)	$Effective\ PCM$ (%)
Room-Temp	MEPCM	30.13	27.59	34.80	143.54	——-
	25%	30.49	27.94	32.69	26.15	18.22
	30%	32.01	27.93	34.49	40.59	28.28
	35%	30.09	27.23	33.43	45.23	31.51
Heated	25%	30.52	26.95	32.73	30.39	21.17

It is important to note the relationship between increasing MEPCM content and resulting effective latent heat of fusion. As the MEPCM content is increased between 25% and 30%, in the room temperature samples, the latent heat of fusion increases by a factor of 1.55, going from 26.15 kJ/kg to 40.59 kJ/kg. Similarly with 25% and 35%, the latent heat of fusion increases by a factor of 1.73, going from 26.15 kJ/kg to 45.23 kJ/kg. It is important to point out that the heated heated 25% sample exhibited a higher latent heat, increasing by a factor of 1.25, going from 26.15 kJ/kg to 30.39 kJ/kg. The peak, onset, and endset temperature values of the mixture appear to remain constant even as the mixture content varies. The samples have an average peak melting temperature of 30.78 °C, an average onset temperature of 27.51 °C, and an average endset temperature of 33.34 °C.

B. Thermal Conductivity

One of the advantages of using LCD printing versus other 3D printing techniques, such as FFF, is the lack of air gaps that normally form, meaning that the functional thermal conductivity of the material should be identical to that of a 3D printed sample that is rigid in geometry. LCD printing produces a smooth surface, which is ideal for TPS testing because it makes certain good thermal contact with the heat source in the setup. Having poor contact with the heating source (Kapton sensor) results in a lower measured thermal conductivity which can lead to skewed results.

Table 2 Average thermal conductivity and standard deviation for each sample ratio

	Sample	k [W/(m-K)]	St.D
Room-Temp	Resin	0.1989	0.0101
	25%	0.2538	0.0066
	30%	0.2593	0.0092
	35%	0.2708	0.0059
Heated	25%	0.2557	0.0073

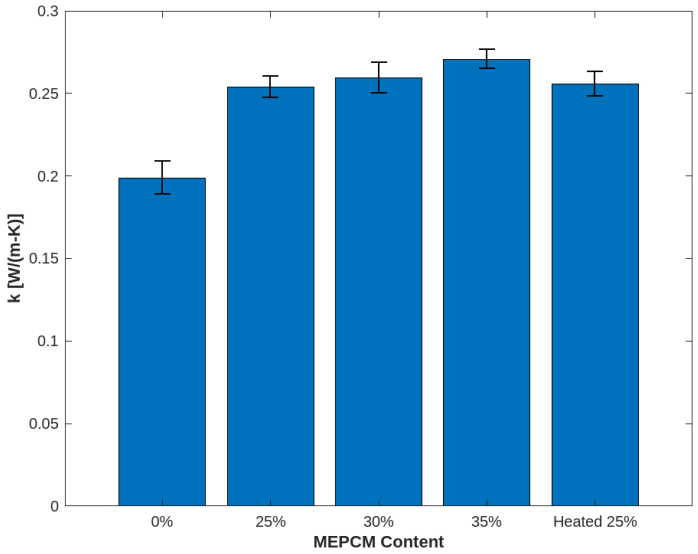

Fig. 3 Average thermal conductivity for each sample. The error bars shown represent the standard deviation

To determine an average effective thermal conductivity and standard deviation for each MEPCM/Resin ratio, each sample was measured twenty times. The resulting thermal conductivity measurements can be seen in Table 2 and Fig. 3. Based upon the results, it can be seen that the addition of MEPCM results in an increase in thermal conductivity. The pure resin has an average thermal conductivity of 0.1989 W/m-K while 25% has an average thermal conductivity of 0.2538 W/m-K. The mixture containing the optimal amount of MEPCM for TES, 35%, was found to have an average thermal conductivity of 0.2708 W/mK. It is worthy to point out that the heated sample of the 25% composite showed slightly higher thermal conductivity with an average conductivity of 0.2557 W/m-k. While the thermal conductivity is still low for heat transfer applications, it may be enhanced using conductivity-enhancing additives and accounting for it in the design of the geometry. Enhanced heat transfer performance can be obtained by accounting for the low thermal conductivity with thinner design fins/walls and higher surface-area-to-volume ratios.

C. Print Quality and Resolution

Another advantage of using LCD printing compared to other 3D printing methods is the ability to get more accurate and precise prints when evaluated against the original CAD model. LCD additive manufacturing techniques print each layer, with each layer being usually 0.05 mm, allowing for relatively more accurate geometric features, especially features that are round in nature. Using a torture test print, a stress test used on 3D printer that is designed to push the limits of the printer's capabilities. By performing a visual inspection and dimensional analysis on the torture test printed in both pure resin and MEPCM-resin composite, conclusions could be drawn on the potential to print the previously stated complex geometries that would allow for maximum surface-area-to-volume ratios.

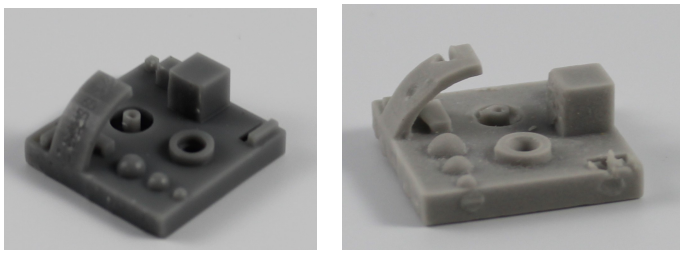

(a) (b)

Fig. 4 Torture test printed at room temperature in pure resin (a) and a 25% MEPCM-resin composite (b)

Upon visual inspection of the samples shown in Figure 4, it was clear that the sample printed in pure resin had a clearer resolution and the debossed numbers were readable. All of the geometric features were printed and looked very

similar to the original CAD model. In contrast, the sample printed of a 25% MEPCM-resin sample had multiple defects such as a hole in the free standing arch and no hole went entirely through the sample print. To determine the average

Table 3 Average percent error of the pure resin and 25% MEPCM-resin composite samples of the torture test print.

	L_{total} (%)	W_{total} (%)	t_{total} (%)	$Cubes$ (%)	$Spheres$ (%)	d_{holes} (%)
Resin	0.080	0.040	0.000	7.667	0.639	0.000
25%	1.04	1.8	3	16.722	5.361	50.750

percent error of both samples, the printed geometrical features were measured using a dial caliper and the difference relative to the original CAD model dimensions were calculated. Then the percent error was then calculated for each size of the feature and then the average was calculated for each group of features, such as cubes and spheres. These results are displayed in Table 3. The pure resin print had below 1% error in most of the dimensions of the features. The largest error was seen in the sizes of the cubes, most likely due to the orientation of the print when sliced for printing. The 25% Room Temperature composite sample however, had greater error in the dimensions of each of the geometrical features. The highest error was seen to be the holes, that were one average less than half way through the sample, and the cubes, which experienced an average of 16.722% error.

V. Concluding Remarks

In the present study, MEPCM was suspended in photocurable resin, creating a composite material for use in LCD 3D printing. Samples of increasing MEPCM contents such as 25%, 30%, 35%, and a sample of 25% heated to 65 °C were 3D printed and explored as a material suitable and capable for TES. DSC testing was used to determine the TES capability of each of the printed samples and it was determined that 35%, the highest achievable MEPCM content, effectively behaves as if there was 31.51% MEPCM in the composite material. The DSC results also showed <1% variation across different sampling regions in the geometry. The thermal conductivity was determined using a TPS. This testing found that the addition of MEPCM results in a general increase in thermal conductivity when compared to that of pure resin. Visual inspection and dimensional anaylysis were used on a sample stress test print in pure resin and 25% MEPCM-resin composite to determine quality of the samples printed and gain a numerical understanding of the errors seen in printing with the MEPCM composite resins.

While the LCD 3D printing process of the mixtures provided lower amounts of difficulties compared to other techniques, there is a very vital limiting factor that currently prevents higher MEPCM ratios from being obtained. The increasing viscosity that occurs with the higher ratios prevents the LCD printers from effectively printing the samples using the present technique. As seen in the quality and resolution testing, composite resin prints made with the unheated mixtures showed many areas of defects or failures. During the creation of the test samples used in this study there were a multitude of failed or faulty prints. A solution briefly tested in this current study was the heating of the composite resin to reduce the number of errors in printing.

Having the composite resins heated in this study have shown that they can lead to more efficient printing and increased latent heat of fusion and thermal conductivity, vital qualities needed for TES. Comparisons between the tested non-heated and heated 25% MEPCM-resin composite samples showed a 16.2 % increase in effective PCM content and a 0.749 % increase in thermal conductivity. The heated samples were also observed to print with minimal defects or failures. Future work will continue to focus on the reducing viscosity of the composite resins through pre-heating the resin before printing and then having the vat and print bed heated during the manufacturing process. This will not only increase the quality of the printed samples, but also increase their thermal energy storage capabilities. Work is needed on streamlining the process and equipment used in controlling the temperature during printing. This would allow for further testing of the heating process and techniques in order to verify the validity of this solution to the high viscosity of the MEPCM-resin composites.

Acknowledgments

This material is based upon work supported in part by the National Science Foundation under Grant number 2050887 and the Embry-Riddle Aeronautical University Department of Mechanical Engineering. Research was preformed under

the guidance and tutelage of Dr. Sandra Boetcher, Isabel Melendez, and Karl Morgan as part of a Research Experience for Undergraduates Internship. These mentors provided the previous research completed and assistance on how to continue forward via new methods and testing. All tests and data reported were preformed by the author and do not necessarily reflect the views of the Embry-Riddle Aeronautical University Department of Mechanical Engineering. The opinions, findings, and conclusions, or recommendations expressed are those of the author and do not necessarily reflect the views of the National Science Foundation and Embry-Riddle Aeronautical University.

References

[1] Navarro, L., de Gracia, A., Niall, D., Castell, A., Browne, M., McCormack, S. J., Griffiths, P., and Cabeza, L. F., "Thermal energy storage in building integrated thermal systems: A review. Part 2. Integration as passive system," *Renewable Energy*, Vol. 85, 2016, pp. 1334–1356. https://doi.org/10.1016/j.renene.2015.06.064.

[2] Navarro, L., de Gracia, A., Colclough, S., Browne, M., McCormack, S. J., Griffiths, P., and Cabeza, L. F., "Thermal energy storage in building integrated thermal systems: A review. Part 1. active storage systems," *Renewable Energy*, Vol. 88, 2016, pp. 526–547. https://doi.org/10.1016/j.renene.2015.11.040.

[3] Morovat, N., Athienitis, A. K., Candanedo, J. A., and Dermardiros, V., "Simulation and performance analysis of an active PCM-heat exchanger intended for building operation optimization," *Energy and Buildings*, Vol. 199, 2019, pp. 47–61. https://doi.org/10.1016/j.enbuild.2019.06.022.

[4] Kalnæs, S. E., and Jelle, B. P., "Phase change materials and products for building applications: A state-of-the-art review and future research opportunities," *Energy and Buildings*, Vol. 94, 2015, pp. 150–176. https://doi.org/10.1016/j.enbuild.2015.02.023.

[5] Alehosseini, E., and Jafari, S. M., "Micro/nano-encapsulated phase change materials (PCMs) as emerging materials for the food industry," *Trends in Food Science Technology*, Vol. 91, 2019, pp. 116–128. https://doi.org/10.1016/j.tifs.2019.07.003.

[6] Suamir, I. N., Rasta, I. M., Sudirman, and Tsamos, K. M., "Development of Corn-Oil Ester and Water Mixture Phase Change Materials for Food Refrigeration Applications," *Energy Procedia*, Vol. 161, 2019, pp. 198–206. https://doi.org/10.1016/j.egypro.2019.02.082.

[7] Lu, W., and Tassou, S., "Characterization and experimental investigation of phase change materials for chilled food refrigerated cabinet applications," *Applied Energy*, Vol. 112, 2013, pp. 1376–1382. https://doi.org/10.1016/j.apenergy.2013.01.071.

[8] Ma, Z. X.-J. J. H. L. D. X., K., and Xie, W., "Application and research progress of phase change materials in biomedical field," *Biomaterials Science*, Vol. 9(17), 2021, pp. 5762–5780. https://doi.org/10.1039/d1bm00719j.

[9] Mondieig, D., Rajabalee, F., Laprie, A., Oonk, H. A., Calvet, T., and Cuevas-Diarte, M. A., "Protection of temperature sensitive biomedical products using molecular alloys as phase change material," *Transfusion and Apheresis Science*, Vol. 28(2), 2003, pp. 143–148. https://doi.org/10.1016/s1473-0502(03)00016-8.

[10] Indirani, S., and Arjunan, S., "Selection and synthesis of thermal energy storage PCM with silicon carbide for biomedical applications," *Applied Nanoscience*, Vol. 12(10), 2022, pp. 2915–2922. https://doi.org/10.1007/s13204-022-02584-6.

[11] Mohamed, S. A., Al-Sulaiman, F. A., Ibrahim, N. I., Zahir, M. H., Al-Ahmed, A., Saidur, R., Yılbas, B., and Sahin, A., "A review on current status and challenges of inorganic phase change materials for thermal energy storage systems," *Renewable and Sustainable Energy Reviews*, Vol. 70, 2017, pp. 1072–1089. https://doi.org/10.1016/j.rser.2016.12.012.

[12] KENISARIN, M., and MAHKAMOV, K., "Solar energy storage using phase change materials," *Renewable and Sustainable Energy Reviews*, Vol. 11(9), 2207, pp. 1913–1965. https://doi.org/10.1016/j.rser.2006.05.005.

[13] Kenisarin, M. M., "Thermophysical properties of some organic phase change materials for latent heat storage. A review," *Solar Energy*, Vol. 107, 2014, pp. 553–5575. https://doi.org/10.1016/j.solener.2014.05.001.

[14] Umair, M. M., Zhang, Y., Iqbal, S., K.a nd Zhang, and Tang, B., "Novel strategies and supporting materials applied to shape-stabilize organic phase change materials for thermal energy storage–A review," *Applied Energy*, Vol. 235, 2019, pp. 846–873. https://doi.org/10.1016/j.apenergy.2018.11.017.

[15] Sánchez-Silva, L., Rodríguez, J. F., Romero, A., Borreguero, A. M., Carmona, M., and Sánchez, P., "Microencapsulation of PCMs with a styrene-methyl methacrylate copolymer shell by suspension-like polymerisation," *Chemical Engineering Journal*, Vol. 157(1), 2010, pp. 216–222. https://doi.org/10.1016/j.cej.2009.12.013.

[16] Salunkhe, P. B., and Shembekar, P. S., "A review on effect of phase change material encapsulation on the thermal performance of a system," *Renewable and Sustainable Energy Reviews*, Vol. 16(8), 2012, pp. 5603–5616. https://doi.org/10.1016/j.rser.2012.05.037.

[17] Khadiran, T., Hussein, M. Z., Zainal, Z., and Rusli, R., "Encapsulation techniques for organic phase change materials as thermal energy storage medium: A review," *Solar Energy Materials and Solar Cells*, Vol. 143, 2015, pp. 78–98. https://doi.org/10.1016/j.solmat.2015.06.039.

[18] Wong, O. I. S. C., M., and Puri, A., "Convective heat transfer and pressure losses across novel heat sinks fabricated by Selective Laser Melting," *International Journal of Heat and Mass Transfer*, Vol. 52(1-2), 2009, pp. 281–288. https://doi.org/10.1016/j.ijheatmasstransfer.2008.06.002.

[19] Deisenroth, D. C., Moradi, R., Shooshtari, A. H., Singer, F., Bar-Cohen, A., and Ohadi, M., "Review of Heat Exchangers Enabled by Polymer and Polymer Composite Additive Manufacturing," *Heat Transfer Engineering,*, Vol. 39(19), 2017, pp. 1648–1664. https://doi.org/10.1080/01457632.2017.1384280.

[20] T'Joen, C., Park, Y., Wang, Q., Sommers, A., Han, X., and Jacobi, A., "A review on polymer heat exchangers for HVAC applications," *International Journal of Refrigeration*, Vol. 32(5), 2009, pp. 763–779. https://doi.org/10.1016/j.ijrefrig.2008.11.008.

[21] Luckow, P., Bar-Cohen, A., Rodgers, P., and Cevallos, J., "Energy Efficient Polymers for Gas-Liquid Heat Exchangers," *Journal of Energy Resources Technology*, Vol. 132(2), 2010. https://doi.org/10.1115/1.4001568.

[22] Arie, M. A., Shooshtari, A. H., Tiwari, R., Dessiatoun, S. V., Ohadi, M. M., and Pearce, J. M., "Experimental characterization of heat transfer in an additively manufactured polymer heat exchanger," *Applied Thermal Engineering*, Vol. 113, 2017, pp. 575–584. https://doi.org/10.1016/j.applthermaleng.2016.11.030.

[23] Liu, J., Guo, H., Zhi, X., Han, K., L.a nd Xu, Li, B., and Li, H., "Heat-transfer characteristics of polymer hollow fiber heat exchanger for vaporization application," *AIChE Journal*, Vol. 64(5), 2017, pp. 1783–1792. https://doi.org/10.1002/aic.16049.

[24] Raza, G., Shi, Y., and Deng, Y., "Expanded graphite as thermal conductivity enhancer for paraffin wax being used in thermal energy storage systems," *2016 13th International Bhurban Conference on Applied Sciences and Technology (IBCAST)*, IEEE, 2016, pp. 1–12.

[25] Caminero, M., Chacón, J., García-Plaza, E., Núñez, P., Reverte, J., and Becar, J., "Additive Manufacturing of PLABased Composites Using Fused Filament Fabrication: Effect of Graphene Nanoplatelet Reinforcement on Mechanical Properties, Dimensional Accuracy and Texture," *Polymers*, Vol. 11(5), 2019, p. 799. https://doi.org/10.3390/polym11050799.

[26] Wencke, Y. L., Kutlu, Y., Seefeldt, M., Esen, C., Ostendorf, A., and Luinstra, G. A., "Additive manufacturing of PA12 carbon nanotube composites with a novel laser polymer deposition process," *Journal of Applied Polymer Science*, Vol. 138(19), 2020, p. 50395. https://doi.org/10.1002/app.50395.

[27] Almuallim, B., Harun, W. S. W., Rikabi, I. J. A., and Mohammed, H. A., "Thermally conductive polymer nanocomposites for filament-based additive manufacturing," *Journal of Materials Science*, Vol. 57(6), 2022, pp. 3993–4019. https://doi.org/10.1007/s10853-021-06820-2.

[28] Freeman, S. D. C. P. N. R. V., T. B., and Boetcher, S. K., "Phase-Change Materials/HDPE Composite Filament: A First Step Toward Use With 3D Printing for Thermal Management Applications," *Journal of Thermal Science and Engineering Applications*, Vol. 11(5), 2019, p. 054502. https://doi.org/10.1115/1.4042592.

[29] Freeman, T. B., Messenger, M. A., Troxler, C. J., Nawaz, K., Rodriguez, R. M., and Boetcher, S. K., "Fused filament fabrication of novel phase-change material functional composites," *Additive Manufacturing*, Vol. 39, 2021, p. 101839. https://doi.org/:10.1016/j.addma.2021.101839.

[30] Zaheed, L., and Jachuck, R., "Review of polymer compact heat exchangers, with special emphasis on a polymer film unit," *Applied Thermal Engineering*, Vol. 24(16), 2004, pp. 2323–2358. https://doi.org/10.1016/j.applthermaleng.2004.03.018.

[31] Salgado-Pizarro, R., Padilla, J. A., Xuriguera, E., Barreneche, C., and Fernández, A. I., "Novel Shape-Stabilized Phase Change Material with Cascade Character: Synthesis, Performance and Shaping Evaluation," *Energies*, Vol. 14(9), 2021, p. 2621. https://doi.org/10.3390/en14092621.

[32] Singh, P., Odukomaiya, A., Smith, M. K., Aday, S., A.and Cui, and Mahvi, A., "Processing of phase change materials by fused deposition modeling: Toward efficient thermal energy storage designs," *Journal of Energy Storage*, Vol. 55, 2022, p. 105581. https://doi.org/10.1016/j.est.2022.105581.

[33] Díaz-Herrezuelo, M.-S. L. M. P. O. M. I., I., and Belmonte, M., "Novel 3D thermal energy storage materials based on highly porous patterned printed clay supports infiltrated with molten nitrate salts," *Additive Manufacturing*, Vol. 59, 2022, p. 103108. https://doi.org/10.1016/j.addma.2022.103108.

[34] Wei, P., Cipriani, C. E., and Pentzer, E. B., "Thermal energy regulation with 3D printed polymer-phase change material composites," *Matter*, Vol. 4(6), 2021, pp. 1975–1989. https://doi.org/10.1016/j.matt.2021.03.019.

[35] Cipriani, C. E., Shu, Y., Pentzer, E. B., and Benjamin, C. C., "Viscoelastic and thixotropic characterization of paraffin/photopolymer composites for extrusion-based printing," *Physics of Fluids*, Vol. 34(9), 2022, p. 093106. https://doi.org/10.1063/5.0104157.

[36] Cipriani, C. E., Ha, T., Defilló, O. B. M., Myneni, M., Wang, C. C., Y.and Benjamin, Wang, J., Pentzer, E. B., and Wei, P., "Structure Processing Property Relationships of 3D Printed Porous Polymeric Materials," *ACS Materials Au*, Vol. 1(1), 2021, pp. 69–80. https://doi.org/10.1021/acsmaterialsau.1c00017.

[37] Gogoi, P., Li, Z., Guo, Z., Khuje, S., An, L., Hu, Y., Chang, S., Zhou, C., and Ren, S., "Ductile cooling phase change material," *Nanoscale Advances*, Vol. 2(9), 2020, pp. 3900–3905. https://doi.org/10.1039/d0na00465k.

[38] Ma, J., Ma, T., Cheng, J., and Zhang, J., "3D Printable, Recyclable and Adjustable Comb/Bottlebrush Phase Change Polysiloxane Networks toward Sustainable Thermal Energy Storage," *Energy Storage Materials*, Vol. 39, 2021, pp. 294–304. https://doi.org/10.1016/j.ensm.2021.04.033.

[39] Roper, C. S., Schubert, R. C., Maloney, K. J., Page, D., Ro, C. J., Yang, S. S., and Jacobsen, A. J., "Scalable 3D Bicontinuous Fluid Networks: Polymer Heat Exchangers Toward Artificial Organs," *Advanced Materials*, Vol. 27z(15), 2015, pp. 2479–2484. https://doi.org/10.1002/adma.201403549.

[40] Jiang, Z., Diggle, B., Tan, M. L., Viktorova, J., Bennett, C. W., and Connal, L. A., "Extrusion 3D Printing of Polymeric Materials with Advanced Properties," *Advanced Science*, Vol. 7(17), 2020, p. 2001379. https://doi.org/10.1002/advs.202001379.

[41] Gupta, C., MB, P., Shet, N. K., Ghosh, A. K., Bandyopadhyay, S., and Mukhopadhyay, P., "Microstructure and mechanical performance examination of 3D printed acrylonitrile butadiene styrene thermoplastic parts," *Polymer Engineering Science*, Vol. 60(11), 2020, pp. 2770–2781. https://doi.org/10.1002/pen.25507.

[42] Melendez, I., Troxler, C. J., Rodriguez, R. M., and Boetcher, S. K., "PHASE-CHANGE MATERIAL SUSPENSION IN PHOTOCURABLE RESIN FOR LIQUID CRYSTAL DISPLAY 3D PRINTING OF THERMAL ENERGY STORAGE COMPOSITES," *Proceedings of the 17th International Heat Transfer Conference, IHTC-17*, IHTC, Cape Town, South Africa, 2023. https://doi.org/10.1615/IHTC17.120-70.